*International Research Journal of Innovations in Engineering and Technology (IRJIET)*

**ISSN (online): 2581-3048**

**Volume 7, Issue 3, pp 106-110, March-2023**

https://doi.org/10.47001/IRJIET/2023.703015

# Effect of Corrugated Inner Surface of a Blade on the Savonius Wind Turbine

**[1]Muhamad Emir Purdiatama, [2]*Khoiri Rozi, [3]Syaiful, [4]Berkah Fajar TK**

[1,2,3,4]Mechanical Engineering, Diponegoro University, Semarang, Jl. Prof. H. Soedarto, SH, Tembalang-Semarang 50275, Indonesia

*Corresponding Author's E-mail: khoiri.rozi@yahoo.com

***Abstract* - This work was conducted to examine the performance and flow characteristics of a Savonius wind turbine with a corrugated inner surface blade. The unsteady 2-D simulation was performed using ANSYS Fluent with a k-ω SST at a wind velocity of 6,2 m/s. The results showed that the flow structure changes with increasing turbine rotation. The corrugated inner surface of the blade causes an increased high-pressure area on the advancing blade. Besides that, the torque and power coefficients are higher than for semicircular standard blades. This value increases as the free-flow velocity increases.**

***Keywords:*** Savonius Wind Turbine, CFD, Corrugated Blade, Coeficcient Power, Coefficient Torque.

## I. INTRODUCTION

The Savonius wind turbine is a vertical-axis wind turbine type that is used to harness wind energy. This turbine has a simple structure, a relatively low operating speed, and the ability to capture wind from all directions. The turbine works based on the drag force difference on the advancing and returning blades so that can produces torque to rotate the turbine[10]. Many parameters that affect turbine efficiency include turbine geometry, especially blade configurations such as blade shape, blade thickness, number of blades, and blade overlap ratio.

Several studies related to the effect of turbine blade geometry have been tested both experimentally and numerically. Patel and Patel [9] vary Savonius blade thickness and found that the thicker the blade, the lower Cp and Ct produced. Shashikumar et. al [12] used a tapered blade and noted a decrease in the value of the Cp turbine. Kerikous & Thevenin [4] and Mahrous [6] modified the blade and noted that can increased turbine torque and power. On the other hand, it is also known that the Cp of the elliptical blade is higher than the Cp of the conventional blade [3]. Mahmoud et. al [10] tested the effect of the overlap ratio from 0 to 0,35 and showed that the turbine without overlap provides higher mechanical power than the turbine with overlap. Shaheen et. al [11] and Meri et. al [8] found that the overlap variation of 0,2 gave the maximum Cp value. A similar study was conducted by Akwa et. al. and shows the maximum Cp reached at e = 0,15[1].

Many aspects of the blades parameters need to be investigated further in order to obtain an optimal work design. The extent to which the influence of shape affects turbine performance is tested in this study through corrugated triangles addition in the concave side of the blades. This study was carried out numerically using the ANSYS FLUENT software package.

## II. METHODOLOGY

### 2.1 Design Geometry

The basic geometry of the turbine was created using the Solid Works 2020 software. The turbine model based on Alom and Saha turbine design which has diameter (D) = 210 mm with overlap ratio (e) = 0,1 and a turbine curvature angle of 180°[2]. Turbine design in 2D for semicircular standard and corrugated blades is shown at Fig.1a and 1b. This simulation using ANSYS fluent with 2-dimensional modeling because it is better to approximate the efficiency of experimental turbine than 3-dimensional modeling [5].

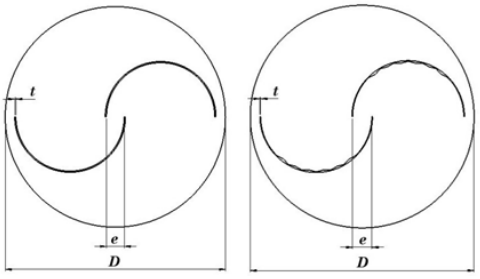


**(a)** **(b)**

**Figure 1: Blade Geometry 2D Model (a) Semicircular Standard (b) Corrugated**

### 2.2 Mesh Generation

The mesh using triangle model with a maximum value of skewness< 0,8 and orthogonal quality > 0,95. The interface between the stationary and rotating domains is equalized by

 

International Research Journal of Innovations in Engineering and Technology (IRJIET)

ISSN (online): 2581-3048

Volume 7, Issue 3, pp 106-110, March-2023

https://doi.org/10.47001/IRJIET/2023.703015

edge sizing to speed up convergence during simulation. To capture the physical phenomena at the boundary layer between the fluid and the blade, inflation layer was created with an average of y+ < 1[3]. Based on the results of the independent grid tests, the number of mesh elements is 320000. The mesh structure is shown in Fig.3.

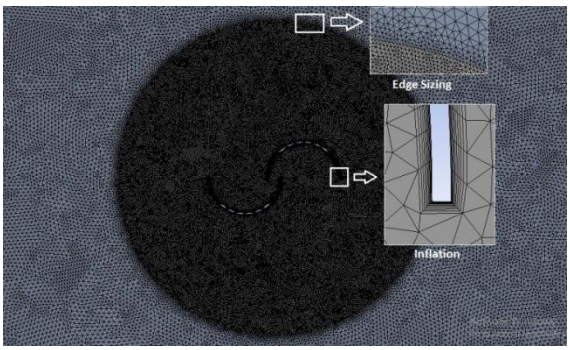


**Figure 3: Mesh Topology**

### 2.3 Boundary Condition and Validation

The boundary conditions are fixed domain, rotating domain, velocity inlet, wall, interface, blades, and pressure outlet, that shown in Figure 3. The size for fixed domains is 6D x 14D and the diameter of the rotating domain is 0,5 m [2]. Two relatively moving mesh zones simulated using sliding mesh with the input wind speed is 6,2 m/s.

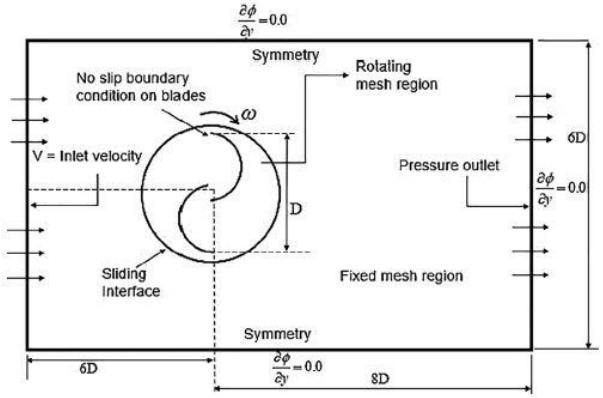


**Figure 4: Geometric Configuration**

CFD method that used is consists of several equations including the momentum and the mass conversion equation. The momentum equation isknown as follows [6]:

$$\rho \frac{Du_j}{Dt} = \rho g_j + \frac{\partial}{\partial x_i}(T_{ij}) \qquad (1)$$

The continuity equation is expressed as:

$$\frac{\partial}{\partial t}(\rho u_j) + \frac{\partial}{\partial x_i}(\rho u_i u_j) = -\frac{\partial P}{\partial x_j} + \rho g_j + \frac{\partial}{\partial x_i}\left[\mu\left(\frac{\partial u_i}{\partial x_j} + \frac{\partial u_j}{\partial x_i}\right)\right] + \frac{\partial}{\partial x_i}\left(-\rho\overline{u_i' u_j'}\right) \qquad (2)$$

The k-omega turbulence with SST model was chosen because it can give results closer to the experiment than other models [12]. K−ω (SST) is formulated in the following equation [7]:

$$\frac{\partial \rho K}{\partial t} + \frac{\partial}{\partial x_j}(\rho v_j K) = \frac{\partial}{\partial x_j}\left[(\mu_L + \sigma_K \mu_T)\frac{\partial K}{\partial x_j}\right] + \tau_{ij}^F S_{ij} - \beta^* \rho \omega K$$

$$\frac{\partial \rho \omega}{\partial t} + \frac{\partial}{\partial x_j}(\rho v_j \omega) = \frac{\partial}{\partial x_j}\left[(\mu_L + \sigma_\omega \mu_T)\frac{\partial \omega}{\partial x_j}\right] + \frac{C_\omega \rho}{\mu_T}\tau_{ij}^F s_{ij} - \beta \rho \omega^2 + 2(1 - f_1)\frac{\rho \sigma_{\omega 2}}{\omega}\frac{\partial K}{\partial x_j}\frac{\partial \omega}{\partial x_j} \qquad (3)$$

The k−ω (SST) model is a combination of the k−ω Wilcox and k−ε turbulence, where the k−ω Wilcox is used in the boundary layer and the k−ε turbulence is used for free shear flow outside the boundary layer.

The power coefficient (Cp) was compared with the Alom result[2]as a numerical validation, and that is shown in the graphic in Fig. 4.

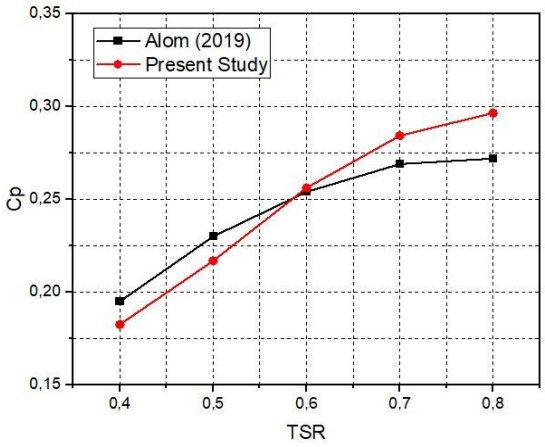


**Figure 5: Validation**

## III. RESULTS AND DISCUSSIONS

### 3.1 Turbine Flow Structure

The velocity flow structure of a semicircular and corrugated blade with rotating angles (θ) = 0° and 90° at tip speed ratio (λ) = 0,8 are shown in Fig. 6 and 7. The various regions in the flow domain were created around the blade profile. The maximum and minimum speed values are represented by the red and blue colors on the bottom side of the plot.As the turbine rotates, the free stream velocity causes the flow to move in a circular pattern around the turbine blades. The flow approaching the turbine separates into two flow areas, one across the convex side of the advancing blade where it is accelerating, and the second stream deflects upward. It shows that the flow is toward the leading edge of the advancing blade and forms a stagnation point for all variation at = 0°. Recirculating flows are formed at the turbine

 

International Research Journal of Innovations in Engineering and Technology (IRJIET)

ISSN (online): 2581-3048

Volume 7, Issue 3, pp 106-110, March-2023

https://doi.org/10.47001/IRJIET/2023.703015

overlap, and high-speed flow is seen on the concave side of the advancing blade. The minimum speed zones are formed around the concave side of the advancing blade and around the convex side of the returning blade. When turbines are at (θ) = 90$^o$, the high-speed flow is formed at the tip of the advancing blade in all variations. Recirculation areas are formed near the turbine overlap and at the leading edge of the returning blade.This is caused by the inward overlap, which plays a role in improving performance mainly due to the flow of air through the gap (e) between the two blades, which inserted pressure drag on the concave side of the returning blade. Fig. 6 and 7 concluded that semicircular and corrugated blades have a similar flow structure.

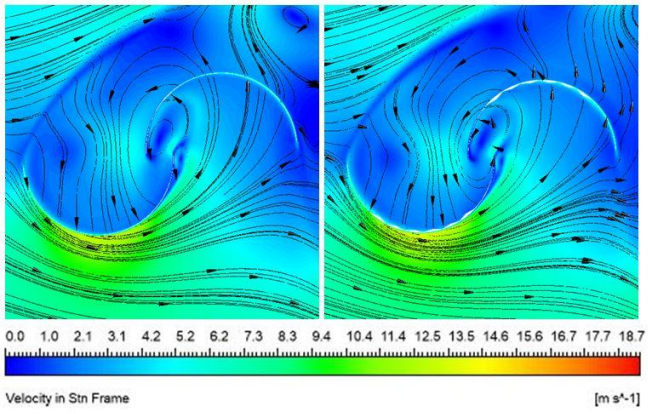


**Figure 6: Velocity Contours of Turbine Savoniusat Rotating Angles (θ) = 0$^o$**

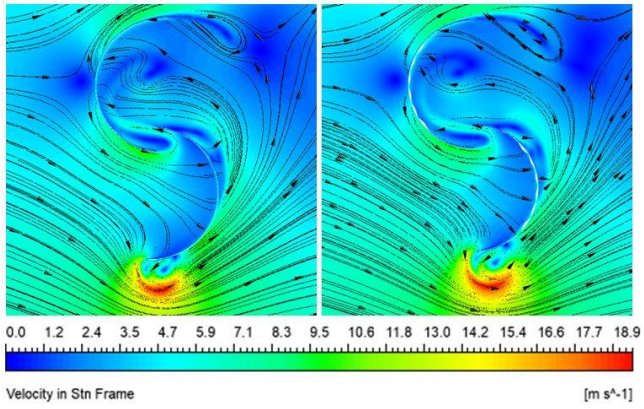


**Figure 7: Velocity Contours of Turbine Savoniusat Rotating Angles (θ) = 90$^o$**

### 3.2 Pressure Distribution

The pressure structure contours of the semicircular and corrugated blade at wind speed V = 6,2 m/s are shown in Fig. 8 and 9. The rotating angles are shown using (θ) = 0° and 90° with a tip speed ratio of (λ) = 0,8. Various regions in the flow domain were created around the blade profile. The maximum and minimum speed values are represented by the red and blue colors on the bottom side of the plot. From the plot, it can be seen that low-pressure and high-pressure areas are formed around the advancing and returning blades. At the turning angle θ = 0$^o$, the high-pressure area at the concave side of the advancing blade and the low-pressure zone around the convex side of the advancing blade are formed. The high-pressure area in a corrugated blade has a bigger pressure than the semicircular blade. When the turning angle θ = 90$^o$, the high-pressure area shifts toward the convex side of the returning blade. The corrugated blade has a higher pressure than a semicircular blade. Moreover, there is a low-pressure area on the trailing edge of the advancing blade. That low-pressure flow zone widens from the convex side of the advancing blade until some portions fill the concave side of the returning blade. Fig. 8 and 9 shows that the modified blade increases pressure on the concave side of advancing blades.

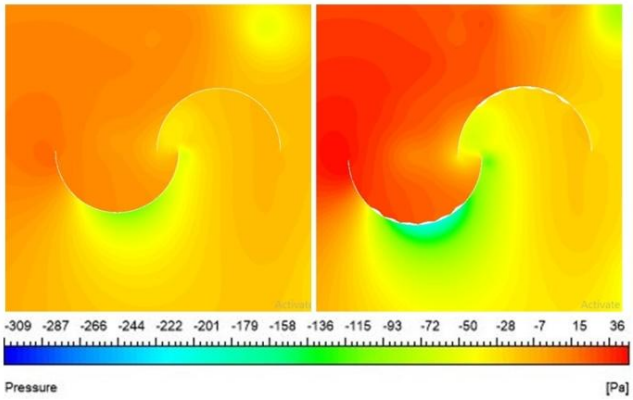


**Figure 8: Pressure Contours of Turbine Savonius at Rotating Angles (θ) = 0$^o$**

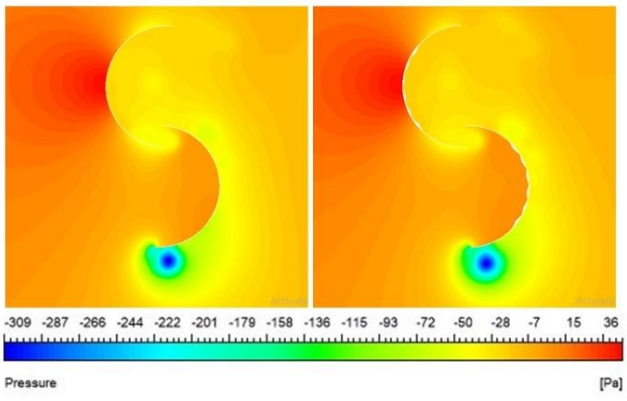


**Figure 9: Pressure Contours of TurbineSavonius at Rotating Angles (θ) = 90$^o$**

### 3.3 Coefficient of Power and Coefficient of Torque

The coefficient power (Cp) and coefficient torque (Ct) was observed to determine the effect of corrugated inner surfaces on blade performance. The results of turbine Cp and Ct with the semicircular and corrugated blades are plotted in the graphs in Fig. 10 and 11. From the plot, it is shown that the turbine Cp value in all variations increases with the increase in

 

International Research Journal of Innovations in Engineering and Technology (IRJIET)

ISSN (online): 2581-3048

Volume 7, Issue 3, pp 106-110, March-2023

https://doi.org/10.47001/IRJIET/2023.703015

TSR. While the average Ct value decreased as the TSR increased. Turbines with the corrugated blade have higher Cp and Ct values at TSR = 0,7 and 0,8. The semicircular and corrugated blades have reached $Cp_{max}$ at TSR = 0,8 with $Cp_{max}$ = 0,272 and $Cp_{max}$ = 0,31 respectively. It can be seen that the corrugated blade contributes to increasing the performance compared to the semicircular blade.

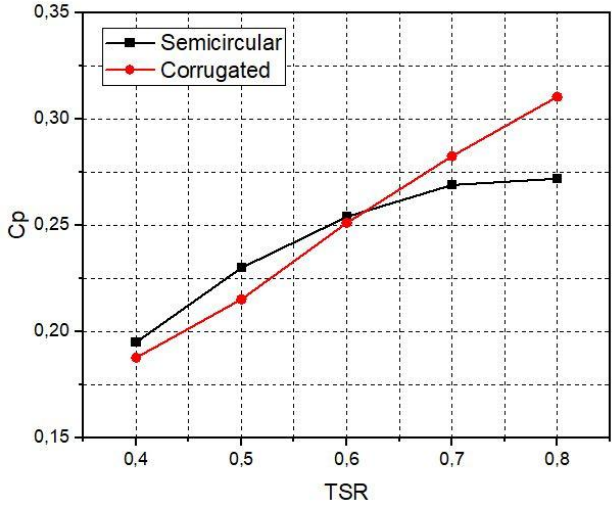


**Figure 10: Coefficient Power with Blade Thickness Variation**

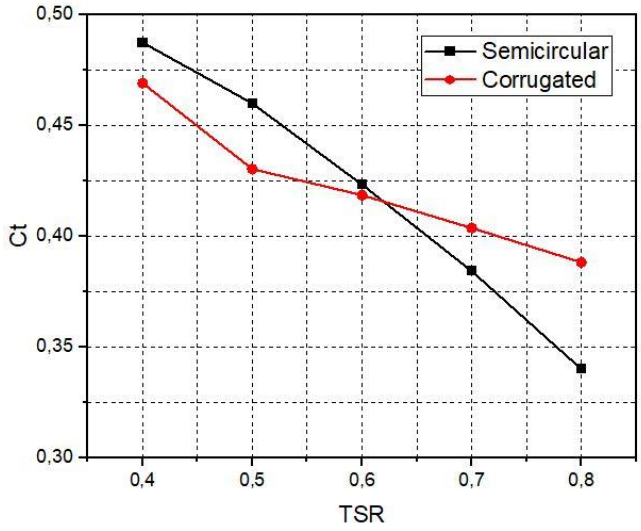


**Figure 11: Coefficient Torque with Blade Thickness Variation**

### 3.4 Coefficient of Torque Static

Simulation results of the semicircular and corrugated blade on Cts at speed v = 6,2 m/s are shown in the graph in Fig. 12. Based on the graph plot for the semicircular and corrugated blades, it can be seen that the low Cts value for the semicircular blade in the range of rotation angle is between $70^o \leq \theta \leq 90^o$ and $250^o \leq \theta \leq 270^o$ with Cts = 0,08 – 0,1. Whereas for the corrugated blade, the range of rotation angles is between $100^o \leq \theta \leq 110^o$ and $270^o \leq \theta \leq 300^o$ with Cts = 0,05 – 0,1. In addition, the high torque for the semicircular blade is obtained in the range of rotation angles between $150^o \leq \theta \leq 175^o$ and $330^o \leq \theta \leq 350^o$ with Cts = 0,63 – 0,68. Moreover, the corrugated blade is in the range of rotation angles between $0^o \leq \theta \leq 30^o$ and $180^o \leq \theta \leq 210^o$ with Cts = 0,65 – 0,7. The high torque occurs because the pressure on the advancing blade is greater than the returning blade. Based on the graphs, it can be seen that the modified blade can produce higher torque than the semicircular blade.

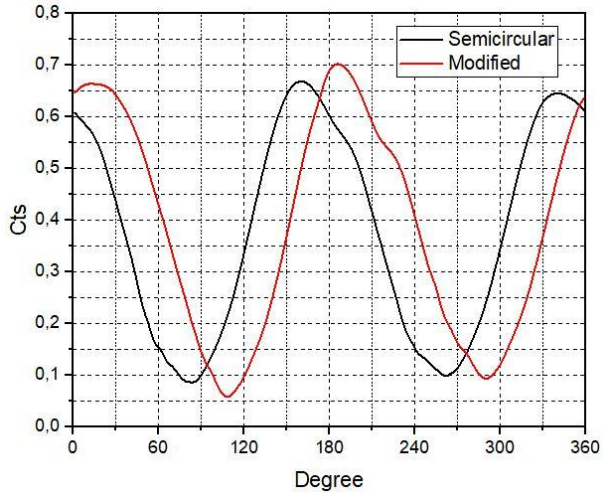


**Figure 12: Coefficient Torque Static (Cts) of Savonius Wind Turbine with Semicircular and Modified Blade**

## IV. CONCLUSION

This simulation examines the effect of modified inner surfaces blade using ANSYS FLUENT. The turbine model was tested with two different blade rotation angles of θ = 0°and 90°. The wind speed used is 6,2 m/s. From the data that has been obtained, it is shown that the value of the torque coefficient (Ct) and the power coefficient (Cp) for modified blade is higher than semicircular blade at TSR = 0,7 and 0,8. This shows that the change in blade shape parameter had the pronounced effect of contributing to raising the efficiency of the Savonius turbine performance compared to the semicircular model.

## REFERENCES

[1] Akwa, J.V., Alves Da Silva Júnior, G. and Petry, A.P. 2012. Discussion on the verification of the overlap ratio influence on performance coefficients of a Savonius wind rotor using computational fluid dynamics. *Renewable Energy*. 38, 1 (2012), 141–149.

[2] Alom, N. and Saha, U.K. 2019. Influence of blade profiles on Savonius rotor performance : Numerical simulation and experimental validation. 186, March (2019), 267–277.

[3] Guo, F., Song, B., Mao, Z. and Tian, W. 2020. Experimental and numerical validation of the influence

 

ISSN (online): 2581-3048
Volume 7, Issue 3, pp 106-110, March-2023
https://doi.org/10.47001/IRJIET/2023.703015

on Savonius turbine caused by rear deflector. *Energy*. 196, (2020).

[4] Kerikous, E. and Thévenin, D. 2019. Optimal shape of thick blades for a hydraulic Savonius turbine. *Renewable Energy*. 134, (2019), 629–638.

[5] Kumar, A., Saini, R.P., Saini, G. and Dwivedi, G. 2020. Effect of number of stages on the performance characteristics of modified Savonius hydrokinetic turbine. *Ocean Engineering*. 217, September (2020), 108090.

[6] Mahrous, A.F. 2021. Computational Fluid Dynamics Study of a Modified Savonius Rotor Blade by Universal Consideration of Blade Shape Factor Concept. *Journal of Advanced Research in Fluid Mechanics and Thermal Sciences*. 85, 1 (2021), 22–39.

[7] Menter, F.R. 1994. Two-equation eddy-viscosity turbulence models for engineering applications. *AIAA Journal*. 32, 8 (1994), 1598–1605.

[8] Meri Al Absi, S., Hasan Jabbar, A., Oudah Mezan, S., Ahmed Al-Rawi, B. and Thajeel Alattabi, S. 2021. An experimental test of the performance enhancement of a Savonius turbine by modifying the inner surface of a blade. *Materials Today: Proceedings*. 42, (2021), 2233–2240.

[9] Patel, V. and Patel, R. 2021. Energy extraction using modified Savonius rotor from Free-flowing water. *Materials Today: Proceedings*. 45, (2021), 5190–5196.

[10] Saad, A.S., Elwardany, A., El-sharkawy, I.I., Ookawara, S. and Ahmed, M. 2021. Performance evaluation of a novel vertical axis wind turbine using twisted blades in multi-stage Savonius rotors. *Energy Conversion and Management*. 235, February (2021), 114013.

[11] Shaheen, M., El-sayed, M. and Abdallah, S. 2015. Journal of Wind Engineering Numerical study of two-bucket Savonius wind turbine cluster. *Jnl. of Wind Engineering and Industrial Aerodynamics*. 137, (2015), 78–89.

[12] Shashikumar, C.M., Vijaykumar, H. and Vasudeva, M. 2021. Numerical investigation of conventional and tapered Savonius hydrokinetic turbines for low-velocity hydropower application in an irrigation channel. *Sustainable Energy Technologies and Assessments*. 43, October (2021), 100871.

**Citation of this Article:**

Muhamad Emir Purdiatama, Khoiri Rozi, Syaiful, Berkah Fajar TK, "Effect of Corrugated Inner Surface of a Blade on the Savonius Wind Turbine" Published in *International Research Journal of Innovations in Engineering and Technology - IRJIET*, Volume 7, Issue 3, pp 106-110, March 2023. Article DOI https://doi.org/10.47001/IRJIET/2023.703015

*******

 